JOURNAL DE PHYSIQUE

Volume 5
Colloque n° 5
Suppl. JP II, n° 6

Proceedings of the Tenth European Conference on Chemical Vapour Deposition

Volume I

ISBN 2-86883-255-5

EPS Recognized by the European Physical Society

Published under the sponsibility of the French Physical Society

sique

Commission paritaire N° 57920.

Directrice de la Publication : Jeanne BERGE

Imprimé en France. — JOUVE, 18, rue Saint-Denis, 75001 PARIS
N° 228616B. Dépôt légal : Août 1995

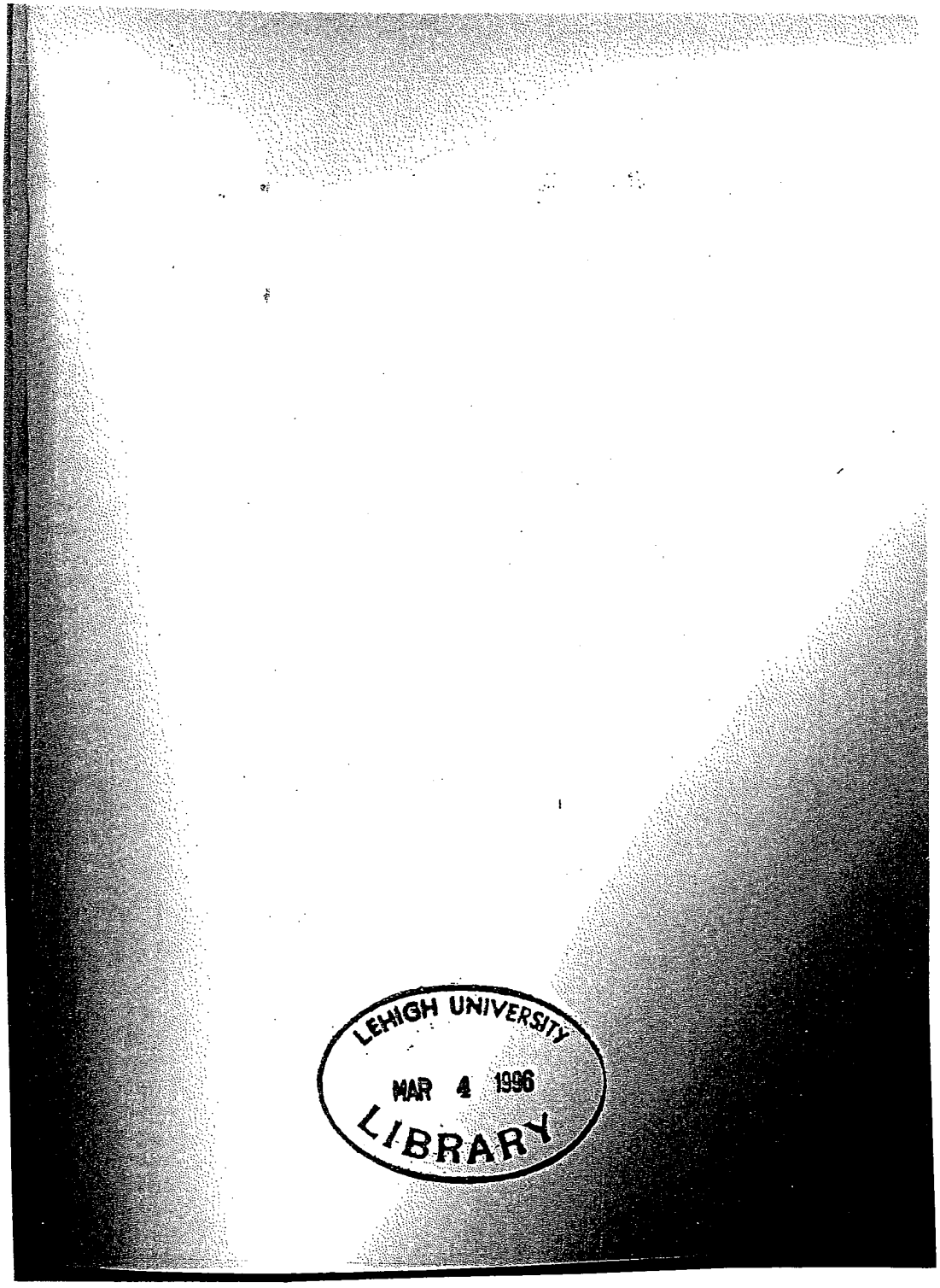
LEHIGH UNIVERSITY
MAR 4 1996
LIBRARY

JOURNAL DE PHYSIQUE IV

Volume 5 | Colloque C5 | Juin 1995

Supplément au Journal de Physique II, n°6

Proceedings of the Tenth European Conference on Chemical Vapour Deposition

Jesolo Lido, Venice, Italy

September 10-15, 1995

Volume I

Edited by: Giovanni A. Battiston
Rosalba Gerbasi
Marina Porchia

Avenue du Hoggar
Zone Industrielle de Courtaboeuf
B.P. 112
91944 Les Ulis cedex A, France

TOYO TANSO TECHNICAL NEWS

1) PERMA KOTE®

Silicon carbide was coated on the isotropic graphite by chemical vapor deposition(CVD)method.
This coating is called PERMA KOTE and its properties are summarized below.

○*A thickness of the coating is ca.120 μm*
(in extreme case it is 1500 μm)
○*Out-gassing from graphite block can be prevented*
○*Low reactivity with corrosive reagent*
○*High resistivity for oxidation*
○*Strong for a thermal shock*
○*Main application is a susceptor of epitaxial growth for Si wafer*

2) SOLSIX®

Composite material composed of graphite and silicon carbide can be manufactured by the reaction between gas phase silicon oxide or liquid phase silicon and graphite.
This composite material is named SOLSIX.
Characteristics of SOLSIX are as follows .
○*C/SiC gradient material or fully SiC can be manufactured*
○*High purity*
○*High resistivity for oxidation*
○*Strong for a thermal shock*
○*Size or shape of the material is freely selected*

3)PYROGRAPH®

Pyrograph is manufactured by the pyrolysis of hydrocarbon on the surface of isotropic graphite.
Characteristics are summarized below.
○*Low permeability for gas and liquid*
○*Increasing surface hardness*
○*Isotropic coating on C/C composite is possible*

TOYO TANSO CO.,LTD.
HEAD OFFICE
7-12,5-CHOME,TAKESHIMA,NISHIYODOGAWA-KU,OSAKA 555,JAPAN
TEL: (06)473-7912 FAX:(06)471-0448
OHNOHARA TECHNICAL DEVELOPMENT CENTER
2181-2,NAKAHIME,OHNOHARA-CHO,MITOYO-GUN,KAGAWA-KEN
769-16,JAPAN
TEL:(0875)-54-2626 FAX:(0875)54-4761

CONTENTS

Volume I

Fundamentals

Growth Modelling

([1])Article not received by the publisher

High T_c Superconductors

MOCVD

CVD History

Volume II

Activated Methods

Ceramics and Coatings

Characterization

New Methods and Materials

Processes for New Industrial Applications

([2]) Article not received by the publisher
([3])Article not received by the publisher

Electronic and Optoelectronic Materials

JOURNAL DE PHYSIQUE IV
Colloque C5, supplément au Journal de Physique II, Volume 5, juin 1995

Chemical Vapor Deposition of ZrO_2 Thin Films Using $Zr(NEt_2)_4$ as Precursor

A. Bastianini, G.A. Battiston, R. Gerbasi, M. Porchia and S. Daolio*

CNR, Istituto di Chimica e Tecnologie Inorganiche e dei Materiali Avanzati, Corso Stati Uniti 4, 35127 Padova, Italy
** CNR, Istituto di Polarografia ed Elettrochimica Preparativa, Corso Stati Uniti 4, 35127 Padova, Italy*

Abstract. By using tetrakis(diethylamido) zirconium [$Zr(NEt_2)_4$], excellent quality ZrO_2 thin films were deposited with high growth rates on alumina and glass substrates by chemical vapor deposition. The depositions were carried out in a hot wall reactor at reduced pressure (200 Pa) in the temperature range 500-580°C and in the presence of oxygen. The as-grown films are colourless, smooth and well-adherent to the substrates. SIMS analysis evidenced pure ZrO_2 with a slight superficial contamination of hydrocarbons and nitrogen. The films have a tapered polycrystalline columnar structure well visible in SEM micrographs. From X-ray diffraction analysis, the monoclinic phase resulted as the major phase together with a small variable amount of tetragonal zirconia. Under 550°C the as-grown films resulted highly textured and were dominated by the (020) orientation. The films were annealed in the range 600-1000°C and the effect of annealing on the texture and on the phase and dimensions of the crystallites have been studied.

1. INTRODUCTION

Zirconia thin films are of considerable interest due to the variety of their applications. In fact, having many peculiar properties such as low electrical conductivity, chemical inertness, permeability, thermal shock resistance and biocompatibility, they can be extensively employed as thermal barrier coatings, oxygen sensors, high-density dynamic memories, buffer layers for high Tc superconducting films, biomedical devices. The precursors used in CVD processes at low temperature both for ZrO_2 films and for zirconium based mixed oxides of technological importance, such as yttrium stabilised zirconia (YSZ) and $Pb(Zr_xTi_{1-x})O_3$ (PZT), had been mainly zirconium alkoxides [1], β-diketonates [2,3] and fluorinated β-diketonates [3,4]. Nevertheless the above precursors may present some drawbacks: in particular alkoxides are very sensitive to hydrolysis, many diketonates are solid at room temperature therefore needing high evaporation temperature and, if fluorinated, could give fluorine contaminations. For this reason we performed depositions of zirconia thin films using a known amido complex of zirconium, $Zr(NEt_2)_4$ as precursor which had already been successfully employed in the CVD growth of Zr_3N_4 in the presence of NH_3 [5]. Amido complexes seem to be promising, suitable and simple sources for CVD of ceramic coatings, other than nitrides, due to their volatility, ease of preparation and handling and because of their ubiquity in the periodic table. In fact amido complexes of almost all metals are known and the deposition of stabilised zirconia starting from analogous amido complexes of zirconium and of the stabiliser metal (i.e. yttrium, lanthanides, alkali metals) could be envisaged.

Large scatter data have been reported concerning the phases obtained in ZrO_2 thin films. However the deposition processes [2,4], the grain size [6] and the thickness [7] seem to play a fundamental role in the nature of the crystalline phases in ZrO_2 thin films. In this paper the effects of both the deposition temperature and the post-deposition annealing on phase distribution, grain size and texture of ZrO_2 films are widely discussed.

2. EXPERIMENTAL

Tetrakis(diethylamido) zirconium was synthesized from $ZrCl_4$ and freshly prepared $LiNEt_2$ (from $HNEt_2$ and LiBu) as reported in the literature [8] and purified by distillation at 112°C/12 Pa. All the operations were carried out in nitrogen filled dry-boxes with rigorous exclusion of oxygen and moisture.

All the ZrO_2 depositions were achieved in a low pressure hot wall CVD reactor where the total pressure, the flow rate, the gas phase composition and the substrate temperature could each be adjusted independently. The depositions were performed on alumina (Morgan-Matroc, Deranox 995) and glass (Corning, barium borosilicate 7059) substrates.

The morphology and thickness of zirconia films were analyzed by Scanning Electron Microscopy (SEM, Philips). Composition analysis was obtained by Secondary Ion Mass Spectrometry (SIMS). The analyses were performed using a custom-built instrument previously described [9]. A mass-filtered duoplasmatron ion gun (VG Fisons, Mod. DP50B), generating a monochromatic (1-10 KeV) O_2^+ or Ar^+ ion beam, coupled to a quadrupole mass analyzer (Balzers A.G., Mod. QMA 400) was used. The samples were bombarded with primary ions at different energy and current density in order to limit surface damage and to perform ion yield optimisation.

X-ray diffraction (XRD) patterns were recorded by a Philips diffractometer PW3710 provided also with a thin film attachment (collimator and flat monocromator) and using $Cu_{k\alpha}$ radiation. The mean grain size was calculated from the peak broadening at full width at half maximum (FWHM) by using the Scherrer formula, where any contributions to broadening due to non uniform strain were ignored,

$$D(nm) = \frac{0.9 \cdot \lambda}{\sqrt{FWHM^2 - B^2} \cdot \cos\vartheta}$$

where D is the mean grain size, λ is the X-ray wavelength (0.15405 for Cu $k_{\alpha 1}$), B is the instrumental broadening and ϑ is the Bragg angle.

3. RESULTS AND DISCUSSION

3.1 Film growth

The use of the liquid $Zr(NEt_2)_4$ has permitted a constant and controllable evaporation rate with respect to the solid $Zr(dpm)_4$ or $Zr(acac)_4$ and has allowed a lower bath temperature (90°C) with respect to the above mentioned precursors i.e. $Zr(dpm)_4$ (230-240°C [2]) and $Zr(acac)_4$ (130-135°C [3,10]), so reducing the experimental difficulties (lower heating of the gas line, less chance of condensation, etc.). This results, together with the ease of preparation and purification of $Zr(NEt_2)_4$ (it can be also be found commercially) and with the purity of the obtained films, justify the choice of an amide as oxide-precursor. On the other hand metal amides have been successfully exploited in MOVPE of III-V semiconductor materials as precursors both for indium and for dopants and the suitability of amides of tin, silicon and tantalum for the low temperature CVD of respective oxides has been recently demonstrated [11].

Deposition of ZrO_2 thin films on Al_2O_3 and glass starting from $Zr(NEt_2)_4$ was achieved in the temperature range 500-580°C. The growth conditions are summarised below:

Deposition Temperature	500-580 °C
Total pressure	200 Pa
O_2 gas flow rate	20 sccm
Carrier gas (N_2) flow rate	150 sccm
Diluting gas (N_2) flow rate	30 sccm
Bath temperature of precursor	90 °C
Molar fraction of precursor	$\cong 3.3 \times 10^{-2}$

The as-grown ZrO_2 films are colourless, smooth and well-adherent to the substrates. The films show a typical columnar grain structure well visible in Fig.1.

Under the above conditions at 550°C the growth rate is 4 μm/h, independently of the substrates; a quite high value if compared with other reported CVD results [2]. The deposition rate increased with an increase of reactor temperature (Fig.2). It is reasonable to hypothesise that the surface chemical reaction is the rate determining process in these conditions. A diminution of the growth rate along the reactor was observed (Fig.2), due to a spatial depletion of the precursor.

Use of different Zr/O ratios influences mainly the uniformity of the deposition along the reactor. In fact using O_2 flow rate 50 or 100 sccm the deposition zone is limited to a few centimeters near the entrance of the reactor giving rise to extremely thick films; in the standard optimised conditions, with O_2 gas flow 20 sccm, the deposition zone is as long as the uniform temperature zone inside the reactor.

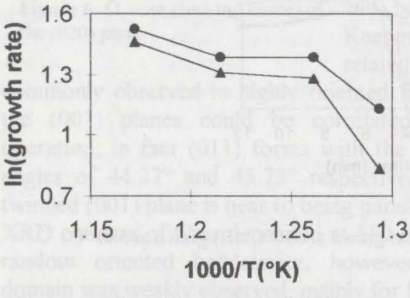

Figure 2 Deposition rates of ZrO_2 versus deposition temperatures at different positions in the reactor: ● 7 cm from the entrance; ▲ 9 cm from the entrance

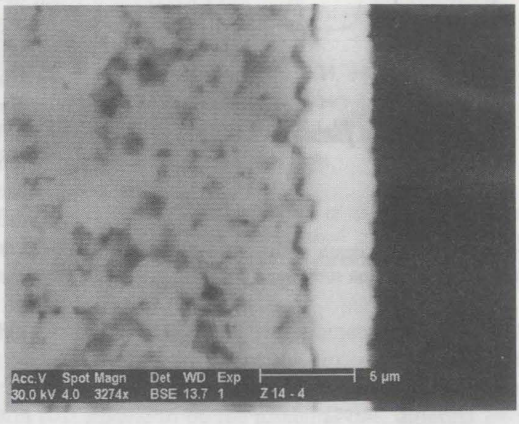

Figure 1: Cross-scctional SEM micrograph of a ZrO_2 film

3.2 SIMS analysis

SIMS was used initially to check the purity of alumina substrates. The obtained results evidence a very intense peak at m/z = 27 (Al^+) and, with very low relative abundances, some peaks corresponding to AlO^+, Al_2^+, Al_2O^+ ion species at m/z = 43, 54 and 70 respectively. Very small amounts of alkaline and earth alkaline metals are evidenced. The high purity of alumina substrates was tested also by in-depth analysis.

Positive ion mass spectra of as-grown ZrO_2 films deposited at the temperatures of 500, 550 and 580°C respectively, show typical isotopic patterns of Zr^+, ZrO^+, ZrO_2^+ and some other peaks with

low intensity originated from organic precursor residuals or contaminants (the most intense isotope of zirconium, ^{90}Zr, has been followed). Fig.3, referring to a sample grown at 580°C, shows the typical in-depth profiles of ZrO^+ (m/z = 106), Zr^+ (m/z = 90), Al^+ (m/z = 27) and of m/z = 13 and 14 due to organic residuals. These last peaks are well evident in the external region, while the m/z = 27 ion profile decreases drastically going from surface to inner layers and increases to a very high value after a long bombardment (≅ 8-9 hours) evidencing an interface region with high ion yields of Al^+, Zr^+ and ZrO^+ species. Interestingly, as the in-depth profiles of the studied samples are very similar, the shapes of the curves obtained in the surface region are quite different for samples deposited at different temperatures. Fig.4 reports such curves for samples grown at 550 and 580°C: the strong differences in the ionic yields of Zr^+ and ZrO^+ on varying the deposition temperature can be seen clearly. This phenomenon can be due to migration of contaminants in the outer layers and/or to different oxide structures.

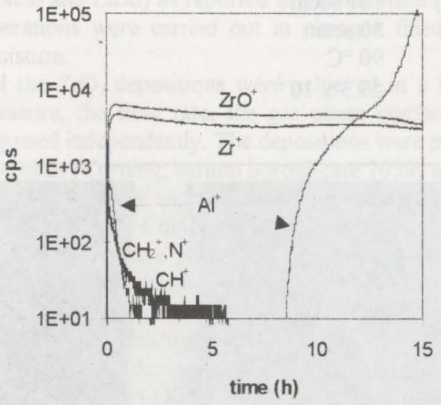

Figure 3 : SIMS depth profile of a ZrO_2 thin film deposited on alumina substrate at 580 °C.

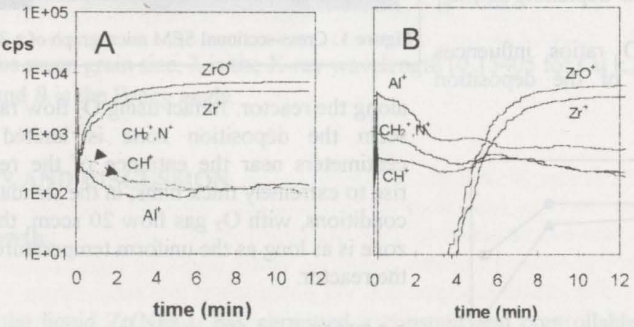

Figure 4 :SIMS depth profile of the superficial layers of ZrO_2 films. (A) grown at 550°C. (B) grown at 580 °C

3.3 XRD studies

X-ray diffraction patterns of as deposited ZrO_2 thin films grown in the temperature range 500-580°C show the reflections of polycrystalline zirconia baddeleyite [12]. Crystallites, random oriented at the highest temperature of 580°C, become gradually oriented with the decreasing of temperature, up to the obtaining of completely textured films at 500 °C (Fig. 5). The intense band at 34.4° in textured films was assigned to the (020) plane as parallel to the substrate according to the following

considerations. X-ray rocking curve (Ω scan) of (020) plane showed a symmetrical distribution with FWHM of about 10° (Fig. 6), indicating a relatively good alignment of the grains along the (020) direction, and a maximum close to the θ value of 17.2°. What's more, the crystallographic planes (031), ($\bar{1}$31), (131) have been taken into account, being the resulting angles β with (020) plane, calculated as 18.88, 23.58 and 27.15° respectively, sufficiently low to make the reflections visible in the XRD patterns. It was possible to check these lines through XRD asymmetric measurements, setting the fixed incident grazing angle as (2θ/2-β).

For the (031), ($\bar{1}$31) and (131) planes it results (55.88°/2-18.88°) = 9.06°, (57.85°/2-23.58°) = 5.34°, (59.77°/2-27.15°) = 2.73° respectively.

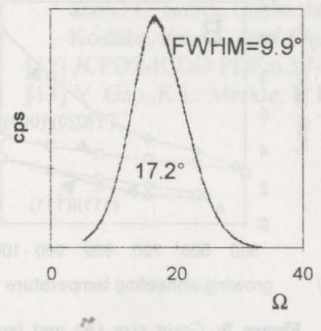

Figure 6: Ω scan (rocking curve) of the (020) plane

In Fig. 7 the 2θ patterns at the fixed incident angles of 2.73° and 9.06° are plotted. The asymmetric geometry measurements are not completely selective either for the closeness of the bands involved or for the spreading of the oriented planes, but the trends confirm (020) plane to be the principal one, different from other depositions reported in literature [4] where the plane (002) was found to be parallel to the substrate.

At deposition temperatures below 550°C besides the intense (020) reflection, the weaker (001), (002) and (003) reflections can be observed, indicating the existence of two domains. Keeping in mind that twin-related grain boundaries are commonly observed in highly oriented films [13], the (020) and the (001) planes could be correlated by a (011) twinning operation; in fact (011) forms with the planes (002) and (020) angles of 44.27° and 45.73° respectively, and in that way the twinned (001) plane is near to being parallel to the (020) plane.

XRD patterns of films deposited at 550 or 580 °C, evidence quite random oriented baddeleyite, however the (111) tetragonal domain was weakly observed, mainly for films located far from the entrance of the precursor in the reactor.

The formation of both the metastable tetragonal phase as already reported in literature [2,7] and random oriented monocline baddeleyite may be related to the fine size of the crystallites. A simple explanation is that tetragonal zirconia phase nucleates and grows first, since it seems there is almost no monoclinic phase in the thinnest films as can be seen in Fig. 8a, while the monoclinic

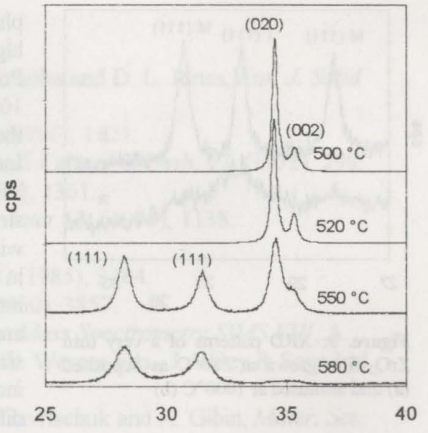

Figure 5: XRD patterns of as-grown ZrO_2 films on glass substrates carried out under different temperatures. Peaks of monocline baddeleyite are marked.

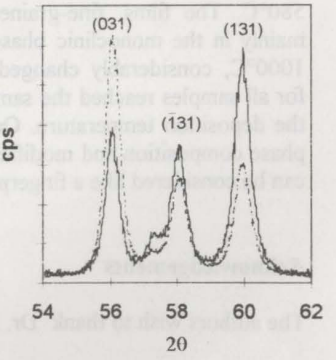

Figure 7: asymmetric patterns with grazing angle of 2.73° (full line) and 9.06° (dotted line)

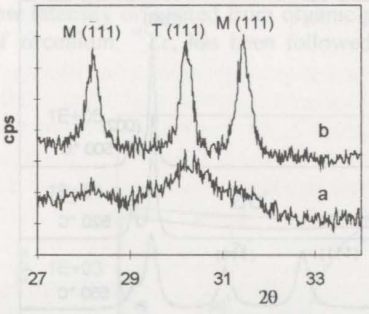

Figure. 8: XRD patterns of a very thin ZrO_2 film grown at 580°C as deposited (a) and annealed at 1000°C (b)

phase was evidenced after the sample was subjected to high temperature (1000°C) treatment (Fig. 8b).

Post deposition annealing in air for three hours in the 600-1000°C temperature range, has only a moderate effect on the zirconia thin films.

Increasing the annealing temperature the diffraction peaks become sharper and stronger in intensity, with a smooth change in the relative peak intensities. After annealing, both grain size and texture increased but to a different extent.

In Fig.9A the dependence of crystallite size on deposition temperature and post-deposition annealing is reported. Whereas the crystallite sizes monotonously decreased increasing the growth temperature, the annealing procedure acted to increase the crystallite sizes up to the same value of about 50 nm. In Fig.9B the ratio between (020) and (002) or between (111) and ($\bar{1}$11) integrated band areas is reported.

Peak area ratios evidenced that samples grown at 520°C were the more textured both as deposited and after annealing.

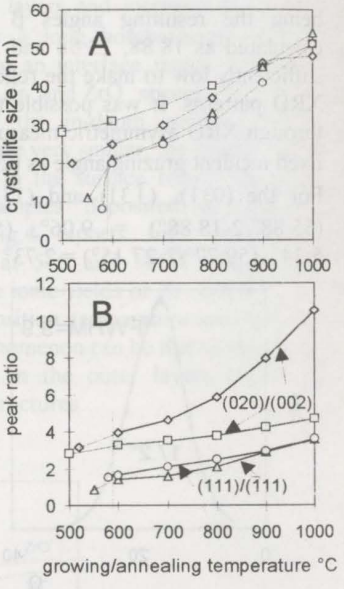

Figure 9: Grain size (A) and band intensity ratios (B); evolution versus annealing temperatures for ZrO_2 thin film deposited at different temperatures. □ 500°C, ◊ 520°C, Δ 550°C, ○ 580°C.

CONCLUSIONS

We have prepared high-quality ZrO_2 thin films from $Zr(NEt_2)_4$ and oxygen with high growth rates in the temperature range 500-580°C. The films, fine-grained and pure, grow polycrystalline mainly in the monoclinic phase. Post-deposition annealing up to 1000°C, considerably changed the crystallite dimensions, which for all samples reached the same value of 50 nm, indipendently of the deposition temperature. On the other hand such a thermal treatment had no influence on the phase composition and modified only slightly the original texture of the films. Therefore the texture can be considered like a fingerprint of a film grown at a particular temperature.

Acknowledgements

The authors wish to thank Dr. P. Guerriero for the SEM measurements.

References

[1] Z. Xue, B. A. Vaartstra, K. G. Caulton, M.H. Chisholm and D. L. Jones, *Eur. J. Solid State Inorg. Chem.*, 29, (1992), 213.
[2] J. Si, S.B. Desu and C.Y. Tsai, *J. Mater. Res.*, 9, (1994), 1721.
[3] M. Balog, M. Schieber, S. Patai and M. Michman, *J. Crystal Growth*, 17, (1972), 298.
[4] C.S. Hwang and H.J. Kim, *J. Mater. Res.*, 8, (1993), 1361.
[5] R. Fix, R.G. Gordon and D.M. Hoffman, *Chem. Mater.*, 3, (1991), 1138.
[6] R.C. Garvie, *J. Phys.Chem.*, 82, (1978), 218.
[7] R.E. Klinger and C.K. Carniglia, *Appl. Optics*, 24, (1985), 3184.
[8] D.C. Bradley and I.M. Thomas, J. Chem. Soc., (1960), 3857.
[9] C. Pagura, S. Daolio, B. Facchin in *Secondary Ion Mass Spectrometry SIMS VIII*, A. Benninghoven, K.T. F. Janssen, J. Tiimpuer, H. W. Werner Eds., J. Wiley & Sons Ltd., 1992, p. 239-242.
[10] N.Dzjubenko, L. Martynenko, N. Zharkova, E. Gavrischuk and A. Gibin, *Mater. Sci. Eng.*, B18, (1993), 232.
[11] L.M. Atagi, D.M. Hoffman, J.R. Liu, Z. Zheng, W.K. Chu, R.R. Rubiano, R.W. Springer and D.C. Smith, *Chem. Mater.*, 6, (1994), 360; T. Tabuchi, Y. Sawado, K. Uematsu and S. Koshiba, *Jpn. J. Appl.Phys.*, 30, (1991), 1974.
[12] JCPDS-ICDD PDF n.37-1484
[13] Y. Gao, K.L. Merkle, H.L.M. Chang, T.J. Zhang and D. J. Lam, *J. Mater. Res.*, 6, (1991), 2417.